Geophysical Research Letters

RESEARCH LETTER
10.1029/2025GL118985

Airborne Radar Reveals Area-Wide Decadal Increase of Surface Mass Balance on the Plateau in Dronning Maud Land, East Antarctica

Alexandra M. Zuhr[1], Steven Franke[1], Olaf Eisen[2,3], Daniel Steinhage[2], Veit Helm[2], Maria Hörhold[2], Johannes Freitag[2], and Reinhard Drews[1]

[1]Department of Geosciences, University of Tübingen, Tübingen, Germany, [2]Alfred Wegener Institute, Helmholtz Centre for Polar and Marine Research, Bremerhaven, Germany, [3]Faculty of Geosciences, University of Bremen, Bremen, Germany

Key Points:

- New radar data show a 21% surface mass balance (SMB) increase in western Dronning Maud Land over the past five decades versus a mean since 1209 C.E.
- Much of the spread in past estimates stems from local variability undersampled by a limited number of firn cores
- Linking firn core data with radar's large-scale coverage is key to capturing SMB changes on centennial and catchment scales

Supporting Information:

Supporting Information may be found in the online version of this article.

Correspondence to:

A. M. Zuhr,
alexandra.zuhr@uni-tuebingen.de

Citation:

Zuhr, A. M., Franke, S., Eisen, O., Steinhage, D., Helm, V., Hörhold, M., et al. (2026). Airborne radar reveals area-wide decadal increase of surface mass balance on the Plateau in Dronning Maud Land, East Antarctica. *Geophysical Research Letters*, *53*, e2025GL118985. https://doi.org/10.1029/2025GL118985

Received 1 SEP 2025
Accepted 30 MAR 2026

Author Contributions:

Conceptualization: Alexandra M. Zuhr, Olaf Eisen, Daniel Steinhage, Reinhard Drews
Data curation: Alexandra M. Zuhr, Steven Franke, Olaf Eisen, Daniel Steinhage, Veit Helm, Maria Hörhold, Johannes Freitag
Formal analysis: Alexandra M. Zuhr, Reinhard Drews
Funding acquisition: Alexandra M. Zuhr, Olaf Eisen, Daniel Steinhage, Reinhard Drews
Methodology: Alexandra M. Zuhr, Steven Franke, Reinhard Drews

Abstract Projections of Antarctica's sea-level contribution depend on future changes in surface mass balance (SMB), yet it remains uncertain whether climate change has already impacted SMB on the East Antarctic Plateau, given diverging trends in prior studies. Using ~3,000 km of airborne radar data from western Dronning Maud Land (DML), we reconstructed SMB over the past ~800 years (1209–2024 C.E.) and found stable centennial averages before 1977, followed by a 21% increase in recent decades. This increase is spatially coherent despite strong small-scale variability driven by topography and wind redistribution, which can bias upscaling of firn core records. Integrating radar and firn core data at ~5 × 5 km^2 scales reduces this bias. Our results show an increase in SMB in western DML over the last five decades. If sustained, it could help mitigate sea-level rise.

Plain Language Summary Antarctica's contribution to sea-level rise depends on its surface mass balance (SMB), which describes how much snow falls and remains on the ice sheet. For East Antarctica's central high-elevated plateau area, it is still uncertain whether present-day climate change has already changed the atmospheric and oceanic conditions and with this the SMB, as previous studies have reported contradictory findings. Here, we studied the ice-internal layering along ~3,000 km of airborne radar data in western Dronning Maud Land. These data allow us to reconstruct SMB over the past ~800 years, from 1209 to 2024. We found that long-term snowfall remained stable, but has increased by 21% during the past five decades. This increase is spatially consistent, although SMB is strongly influenced by environmental factors, such as topography and wind, potentially biasing reconstructions based solely on a few point measurements from firn cores. By combining spatially extensive radar with locally high-resolution firn core data and averaging over larger areas (approximately 5 × 5 km^2), we can reduce SMB uncertainty and improve the reliability of reconstructions. Our results reveal an increase in SMB in western Dronning Maud Land in recent decades, suggesting that if these elevated SMB conditions persist, it could help mitigate sea-level rise.

1. Introduction

The Antarctic Ice Sheet holds ~60%–70% of Earth's freshwater (e.g., Fretwell et al., 2013; Morlighem et al., 2020; Pritchard et al., 2025), and its current mass loss contributes substantially to sea-level rise (e.g., Smith et al., 2020). The future role of the East Antarctic Ice Sheet (EAIS) largely depends on evolving surface mass balance (SMB; defined as the net difference between snow accumulation and losses). SMB changes remain poorly constrained, leading to differing sea-level rise projections (e.g., Payne et al., 2021; Seroussi et al., 2020, 2024; Wirths et al., 2024). Increasing temperatures accelerate mass loss but also enhance snowfall with varying temperature-accumulation sensitivities (Fudge et al., 2016; Nicola et al., 2023). Spatial patterns of increased snowfall differ between coastal areas and the EAIS interior (e.g., Frieler et al., 2015; Kittel et al., 2021). A major challenge is the lack of in situ observations, particularly on the EAIS (Thomas et al., 2017), that provide a common baseline predating anthropogenic warming. Firn cores combined with radar data form the primary archive for bridging this gap.

Reconstructing SMB over decadal to centennial timescales begins with dated snow pits and firn cores. Combined with density-depth profiles, these records provide local specific SMB averaged over intervals defined by age tie points. Considerable progress has been made in placing these point measurements in a regional context using atmospheric or climate models and reanalysis data, operating at resolutions of tens of kilometers (Dalaiden

Project administration: Alexandra M. Zuhr
Supervision: Reinhard Drews
Validation: Alexandra M. Zuhr
Visualization: Alexandra M. Zuhr
Writing – original draft: Alexandra M. Zuhr, Steven Franke, Olaf Eisen, Reinhard Drews

et al., 2021; Eswaran et al., 2024; Monaghan et al., 2006; Medley & Thomas, 2019; D. Wang et al., 2025; Y. Wang & Xiao, 2023). This integration in local-to-continental upscaling efforts allows for direct comparison of recent climate change relative to a centennial baseline, providing the background to assess whether changes in SMB are likely to buffer sea-level rise (Eswaran et al., 2024; Monaghan et al., 2006; Medley & Thomas, 2019; Y. Wang & Xiao, 2023).

A key limitation, particularly in Dronning Maud Land (DML), is that many in situ records often end in the early 2000s (e.g., Anschütz et al., 2011; Eisen et al., 2005; Fujita et al., 2011; Oerter et al., 2000; Rotschky et al., 2004; Y. Wang et al., 2021). Additionally, it remains unclear to what extent spatial SMB variability may overprint temporal trends derived from point measurements. This variability is primarily controlled by wind speed and direction (e.g., Dattler et al., 2019; Eisen et al., 2005; Fujita et al., 2011; Studinger et al., 2020) in interaction with sub-meter-scale surface topography (e.g., Dallmayr et al., 2025; Drews et al., 2015; Hirsch et al., 2023; Zuhr et al., 2021). To separate temporal signals from spatial noise, single-point measurements are often averaged across sites spanning hundreds of kilometers (Rotschky et al., 2004, 2007; D. Wang et al., 2025). Such variability, combined with sparse networks and differing reconstructions, introduces uncertainties in EAIS-wide SMB trends (Eswaran et al., 2024), underscoring the need for extended, high-resolution records.

Here, we present a SMB reconstruction for the past eight centuries (1209–2024) from radar-traced isochrones in airborne ultra-wideband (UWB) data collected on the plateau in western DML (wDML). A key advance is that deep-sounding UWB radar now resolves near-surface stratigraphy at a resolution comparable to earlier ground-based or shallow-sounding airborne surveys. Combined with a nearby firn core, these data offer both large spatial coverage and sufficient temporal resolution to address major observational gaps in DML. We find a substantial SMB increase over the past five decades (~1977–2024) compared to the preceding centennial long-term mean. Using our dense sampling, we quantify the spatial scales at which independent observations are needed to robustly detect such trends and discuss inconsistencies among recent studies.

2. Study Area, Data and Methods

2.1. Polar Plateau in Western Dronning Maud Land

The 3,000 km long flight lines cover elevations between 2,000 and 3,700 m above sea-level (asl) and an area of approximately 150,000 km^2 in wDML on the EAIS (Figure 1a). The flights with the aircraft Polar6 started and/or ended at the German station Kohnen (AWI, 2016a; AWI, 2016b) and the Norwegian station Troll. The lines intersect firn core drilling sites used to reconstruct accumulation rates in the past (e.g., Oerter et al., 2000). The area is characterized by present-day accumulation rates below 200 kg m^{-2} a^{-1} with decreasing trends with increasing elevations (Eisen et al., 2004, 2005). Additionally, we use conductivity and density data from a previously unpublished firn core B52 for data processing (Figures 1a and 1b, Table S1 in Supporting Information S1).

2.2. Derivation of SMB From the Radar Stratigraphy

We follow Koch et al. (2023) and Franke, Steinhage, Helm, Zuhr et al. (2025) using the isochronal radar stratigraphy in combination with conductivity, density and age estimates from firn core B52 to derive a direct proxy for the SMB history and associated uncertainties along the radar profiles (Eisen et al., 2008). We hereby consider both temporal averages from the 2023/24 ice surface to the depth of the respective isochrones and interval estimates between isochrones. Following the shallow-layer approximation (Waddington et al., 2007), we neglect ice dynamic thinning (more details in Text S1 and S2 in Supporting Information S1).

2.3. Geostatistical Metrics for Spatiotemporal Variability

We use multiple metrics to characterize spatial and temporal SMB variability and enable comparison with published accumulation and SMB estimates, accounting for SMB heterogeneity across the EAIS. To quantify temporal uncertainty, we propagate the computed overall uncertainty, that is, the combined uncertainties potentially affecting SMB data, by generating 1,000 realizations using the observed mean and standard error for each sample interval duration (Table S3 in Supporting Information S1). This approach generates probability

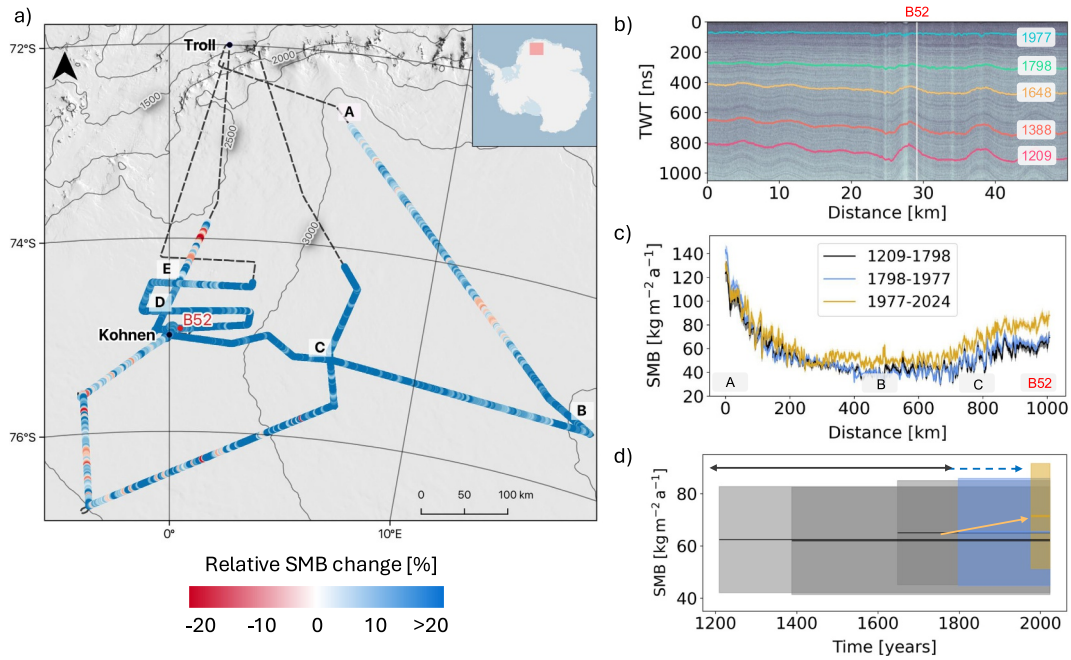

Figure 1. Overview of surface mass balance (SMB) change along radar profiles around Kohnen station shown in (a); dashed black lines illustrate the flight lines colored points the relative SMB change [in %] from the long-term mean (1209–1798) to modern values (1977–2024). Firn core B52 was used for dating and conversion of the two-way traveltime to depth. (b) The profile 20231129_01_008 shows exemplarily the five internal reflection horizons (IRHs, coloured with year of origin C.E.) and the B52 firn core location (vertical white line). (c) SMB visualization for three time periods (black: 1209–1798, blue: 1798–1977, gold: 1977–2024) for one flight line extending from point A via B and C to B52. Solid lines illustrate the mean and shading the combined uncertainties potentially affecting the SMB estimate (Text S2 in Supporting Information S1). The cumulative SMB between each IRH and the surface for all data points is shown in (d), highlighting the long-term mean from 1209 to 1798 (black line) and to 1977 (blue line) as well as the change to modern values during the last five decades (gold, 1977–2024). The shading is the spatial standard deviation of all data points for each period, representing the spatial variability.

distributions for each period and enables robust estimation of 95% confidence intervals and *p*-values when comparing the mean SMB of recent decades (1977–2024) to the long-term baseline.

Spatial variability was characterized by calculating the standard deviation as a measure of SMB heterogeneity across the study area, alongside empirical semivariograms to quantify how semivariance changes with distance. Once the semivariance does not change with distance anymore, at the spatial range where the sill is reached, spatial correlation ceases (Curran, 1988). The *y*-intercept, that is, the nugget, indicates variability smaller than the sampling interval (Bohling, 2005; Curran, 1988). We normalize the semivariance to the respective mean to remove the effect of the absolute SMB values for better comparability and we chose a spherical variogram fit based on the smallest weighted sum of squared error.

The derived spatial range is used to estimate the effective distance between independent observations (Section 3.2), suggesting an exemplary sampling approach that combines radar and baseline data. Additionally, we average randomly drawn data points along flight lines around selected points to quantify the minimum number of observations, for example, radar traces, needed to average small-scale spatial variability relative to the temporal changes in question. We average a varying number of data points (3, 5, 10, 25, 50, 75, 100, 150 and 200) at each location and repeat the calculation 1,000 times to account for spatial variability, each within the spatial range determined by the semivariogram.

3. Results

3.1. Relatively Stable SMB Conditions in wDML Prior to 1977

We derived SMB from five traced internal reflection horizons (IRHs) in airborne UWB radar data for the plateau area in wDML (Figures 1a and 1b). The IRHs are dated (CE) to 1977 (±2 years), 1798 (±7 years), 1648

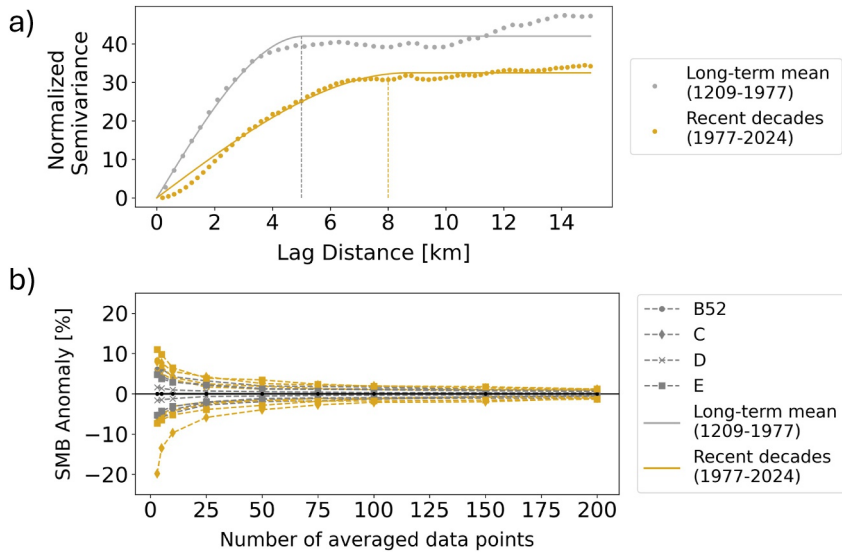

Figure 2. Assessment of data requirements for reliable surface mass balance (SMB) reconstructions. (a) Empirical semivariogram of radar-derived SMB data shows normalized semivariance versus distance for the long-term mean (1209–1977; gray) and the past five decades (1977–2024; gold). Vertical dashed lines indicate the respective distance, that is, range, for both periods. (b) illustrates SMB anomalies [%] relative to the local mean at four locations (Figure 1a) when averaging variable numbers of randomly sampled points within a 2.5 km radius for the long-term mean (1209–1977; gray) and the recent decades (1977–2024; gold). Points represent means of 1,000 calculations per number of averaged data points.

(±11 years), 1388 (±16 years) and 1209 (±19 years), covering a time span of ∼800 years (Figure 1b). The shortest period spans 47 years from 1977 to 2024, and the longest 260 years from 1388 to 1648. We investigate SMB estimates between the surface and each IRH as well as averages between consecutive IRHs.

We observed SMB higher than 130 kg m^{-2} a^{-1} at lower elevated areas (below 2,900 m asl north of Kohnen station) and values below 50 kg m^{-2} a^{-1} at higher elevations toward the interior of the plateau (above 3,300 m asl, Figure 1c). The spatially averaged SMB values from 1209 to 1798, 1209 to 1977 and 1798 to 1977 converge to a long-term mean of 59 kg m^{-2} a^{-1}, with spatially averaged values fluctuating within a relatively narrow range of 52–65 kg m^{-2} a^{-1} (Figure S5, Table S2 in Supporting Information S1). We therefore interpret SMB in wDML between the 13th and the late 20th century as comparatively stable within this bounded range. Standard deviations for the pre-1977 periods are comparable (18–19 kg m^{-2} a^{-1}), indicating similar spatial SMB variability across the study area during this period.

3.2. Recent SMB Increase Over the Past Five Decades

Over the past five decades, we observed an increase in SMB of 21% compared to our chosen baseline periods, 1209–1798 and 1209–1977 (Figure 1d). SMB changed on average by 12 kg m^{-2} a^{-1} to 71 kg m^{-2} a^{-1}, compared to the long-term mean of 59 kg m^{-2} a^{-1}. This increase relative to the long-term mean is observed at 92% of all data points and remains consistent across spatial variations (Figure 1a), such as the divide toward point B and the strong increase north of Kohnen station. The magnitude of change varies spatially and is independent from the baseline SMB (Figure 1c, Figures S2–S4 in Supporting Information S1). The uncertainty quantification described in Section 2.3 indicates that mean SMB in recent decades is higher than the long-term mean. Taking into account the calculated uncertainties (Text S2, Table S3 in Supporting Information S1), the 95% confidence interval (3.69–18.98 kg m^{-2} a^{-1}) and the p-value ($p = 0.006$) indicate that this increase is considered statistically significant; however, the result is highly sensitive to the chosen temporal baseline which differs in different studies.

Firn cores contain precise information on temporal SMB changes at point locations, but their absolute SMB values are sensitive to the specific sampling location. Our radar-derived SMB data show that spatial variability often exceeds the magnitude of temporal changes observed in our study area (Figure 1c). More specifically, the semivariogram's classical shape (Figure 2a) reveals that, over distances shorter than 5 km, the signal is primarily dominated by variability caused by small-scale topographic features. This effect is stronger for the long-term

mean than for the recent decadal average which shows a lower sill and a larger range. In both cases the nuggets are indistinguishable from zero indicating the absence of unknown smaller-scale processes beyond the resolution of the radar data.

To assess the influence of sampling location, we averaged a variable number of radar-inferred SMB estimates in a 2.5 km radius at four selected sites with robust data coverage and different SMB levels (Figures 1a and 2b). This radius was chosen based on the approximately 5 km spatial correlation range inferred from the semivariogramm of the long-term mean (Figure 2a). By analyzing anomalies, we removed the dependence on absolute SMB values and facilitated direct comparison among sites. Even when averaging more than ten randomly selected samples, the spatial variability remained within ±10 % which is comparable in magnitude to the observed temporal change. This indicates that absolute SMB values from individual firn cores should best be averaged over several kilometers of radar profiles to obtain a representative regional SMB value. Considering such an uncertainty when using only firn core-derived SMB estimates in the form of absolute values, this can result in a significant bias during upscaling. Relative values of temporal changes are more robust because they rely only on the differences over time.

4. Discussion

4.1. Temporal Context and Robustness of the Recent SMB Increase

Previous SMB reconstructions on the plateau in wDML were primarily constrained by snow pits, firn cores and local ground-based radar surveys near the EPICA drilling site and Kohnen station (e.g., Altnau et al., 2015; Anschütz et al., 2009, 2011; Eisen et al., 2005; Hofstede et al., 2004; Oerter et al., 1999, 2000; Rotschky et al., 2004, 2007; Winton et al., 2024). Most studies did not detect clear SMB trends during the late 20th century. Notably, Medley et al. (2018) reported a distinct increase after 1980 based on the annually resolved firn core B40 drilled near Kohnen station in 2010. In contrast, Winton et al. (2024), analyzing the ISOL-ICE firn core located ∼1 km from B40, found no significant accumulation change over their record ending in 2017 (core locations in Figure S6 in Supporting Information S1). The discrepancy likely reflects small-scale spatial heterogeneity that can mask temporal trends in single-point records.

Recent local-to-continental upscaling studies based on largely identical firn core networks nevertheless reported substantially differing 20th-century SMB patterns, reflecting methodological differences in spatial interpolation, coherence patterns and baseline definitions (e.g., Eswaran et al., 2024; Medley & Thomas, 2019; Y. Wang & Xiao, 2023). Notably, Eswaran et al. (2024) found no significant trend for 1901–2000 but a positive trend for 1970–2000, broadly consistent with the timing of the increase detected here. Many of these reconstructions end in the early 2000s, leaving the most recent decades unconstrained. Satellite gravimetry and altimetry data (e.g., GRACE and GRACE-FO) indicate a net mass gain in wDML during the 21st century (Velicogna et al., 2020; W. Wang et al., 2025), supporting the positive anomaly observed in our radar-derived SMB record.

Our spatially averaged radar-based reconstruction extends to 2024 and indicates a robust 21% SMB increase over 1977–2024 relative to the baselines 1209–1798 or 1209–1977. Our analysis does not resolve a continuous temporal trend, but rather documents a difference between the post-1977 interval and the preceding long-term mean. The averaged product provides a first-order wDML SMB estimate that transparently reflects the spatial coverage of radar observations, rather than a fully interpolated geostatistical product. Moreover, this approach should be interpreted as observation-constrained rather than representing every sub-region equally.

To enable consistent comparison between different reconstructions, we recalculated our record, both firn cores (B40, ISOL-ICE) and two large-scale reconstructions from Medley and Thomas (2019) and Eswaran et al. (2024) relative to a common reference period (1801–1976 for firn cores and reconstructions, 1798–1976 for the radar data) and standardized each time series using its own mean and standard deviation (Figure 3). For the upscaling reconstructions, we extracted only the fraction overlapping the radar survey area in wDML to ensure spatial consistency. The comparison illustrates both the change after 1977 and its magnitude relative to multi-century variability. The post-1977 radar anomaly exceeds most multi-decadal fluctuations during the preceding centuries, indicating a sustained increase of the most recent period average relative to the long-term mean.

Despite being separated by only ∼1 km, both firn cores exhibit contrasting late 20th-century trends (Figures 3a and 3b), underscoring the influence of small-scale variability. Consistent with this, variability is largest in the individual cores, intermediate in the reconstructions and smallest in our spatially averaged radar record.

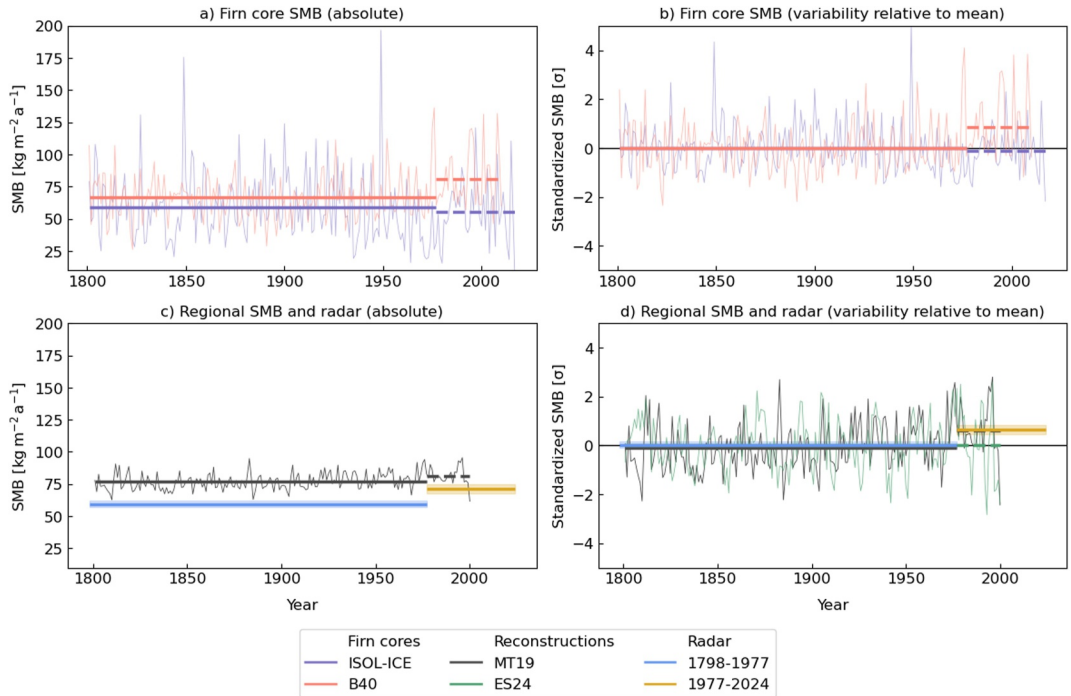

Figure 3. Surface mass balance (SMB) variability from firn cores, upscaling reconstructions and radar estimates in wDML. In all plots are solid lines indicating annual values, horizontal lines period means with a solid line for the early phase and a dashed line for the period after 1977. (a) shows annual SMB from the ISOL-ICE and B40 firn cores with horizontal lines indicating period means for 1801–1977 and 1977–2010 (B40, Medley et al. (2018)) or 1977–2017 (ISOL-ICE, Winton et al. (2024)). In (b) the same records are standardized relative to the 1801–1976 mean and standard deviation; the black line marks zero. Regional SMB reconstruction (MT19) and radar-derived SMB for 1798–1976 and 1977–2024 are shown in absolute units in (c). Shaded bands show $\pm 1\ \sigma$ uncertainty from the radar data. In (d), standardized regional reconstructions (MT19 and ES24) and radar estimates relative to the 1801–1976 baseline are presented. All standardized values are expressed in units of σ computed from the 1801–1976 reference period. MT19 corresponds to Medley and Thomas (2019) and ES24 to Eswaran et al. (2024).

Nevertheless, the divergence among records in both magnitude and standardized variability underscores the challenges of deriving regionally representative SMB trends within DML and emphasizes the value of spatially integrated radar observations for reconciling local and large-scale estimates.

4.2. Catchment-Dependent SMB Trends Across the East Antarctic Plateau

The larger-scale SMB variability across our study area (>20 km) is primarily driven by broad surface elevation gradients and the associated wind system. On sub-kilometer scales, the spatial variability is within 10%–20%, often linked to surface roughness in previous studies (e.g., Anschütz et al., 2011; Fujita et al., 2011; Karlöf et al., 2005; Rotschky et al., 2004). In our study, SMB extrema are vertically aligned (Figure 1b) suggesting that this surface roughness is temporally stable and likely reflects persistent ice flow over corresponding bedrock undulations (Budd & Carter, 1971; Robinson, 1966; Rotschky et al., 2004). These topographic effects lead to increasingly pronounced variability with depth, because corresponding synclines and anticlines in the radar stratigraphy cumulatively increase in amplitude with depth and hence time. This interpretation is supported by the structure of the semivariograms from the different time periods (Figure 2a), indicating ranges between 5 and 8 km. To mitigate the influence of local variability and enhance the robustness of SMB reconstructions, we recommend spatial averaging over approximately 5×5 km^2 grid cells in wDML using radar-derived SMB estimates. In regions with different surface topography conditions, grid cell sizes may need adjustment, which can be evaluated on a case-by-case basis using radar data.

In the broader context of the EAIS, recent regional SMB changes show notable spatial variability. Ground-based radar data from areas further east toward Dome Fuji indicate no significant SMB increase during the 19th and 20th centuries (Müller et al., 2010), while Fujita et al. (2011) found substantially higher SMB in the second half of the

20th century compared to the past 700 years in a similar sector. In Princess Elisabeth Land, SMB reconstructions from stake arrays from Zhongshan station to Dome A indicate decreasing SMB between 2005 and 2020 (D. Wang et al., 2025). Additionally, large-scale reconstructions show substantial spatial variability (e.g., Eswaran et al., 2024; Medley & Thomas, 2019; Y. Wang & Xiao, 2023). Together with our findings from wDML, these studies suggest spatial variability across the EAIS, with increases near the EPICA DML drilling site (Atlantic sector) and recent declines toward Princess Elisabeth Land (Indian sector), a pattern that may be shaped by variations in atmospheric circulation, moisture supply and topographic influences, such as elevation and slope.

5. Conclusions

We used airborne UWB radar data to map large-scale near-surface stratigraphy and reconstruct SMB in wDML on the EAIS over the past 800 years. Our results showed a 21% increase in SMB over the past five decades (1977–2024) relative to the 1209–1798 and 1209–1977 baselines, demonstrating an increase relative to previous centuries.

The comparison of radar-derived SMB with nearby firn cores and large-scale reconstructions demonstrates that single-point records can display contrasting late 20th-century trends, even within kilometer-scale distances. In contrast, the spatially integrated radar record yields a more muted but coherent signal, highlighting the importance of spatial averaging for detecting catchment-scale changes.

The extended temporal coverage of our data set, reaching until 2024, likely accounts for part of the discrepancy between previous studies and our new observations, as records from earlier studies ended in the early 2010s. By combining multi-century coverage with spatially extensive observations, our study strengthens the evidence for a recent SMB increase in the Atlantic sector of the EAIS and underscores the value of airborne radar for bridging local and regional SMB records. Further improvements in temporal resolution will be essential to constrain the onset of the recent increase relative to earlier conditions and to better link SMB variability to atmospheric circulation changes.

Conflict of Interest

The authors declare no conflicts of interest relevant to this study.

Availability Statement

Radargram quicklooks and accompanying metadata of AWI's airborne radar data are available in the *Radar Data over Polar Ice Sheets viewer* of the Marine Data Portal (https://marine-data.de/viewer/; Franke, Steinhage, Helm, Binder et al., 2025). Processed radar data products are available on PANGAEA (https://doi.org/10.1594/PANGAEA.972094; Eisen et al., 2024). The radar data from the *SnACC DML* campaign used in this sstudy can be downloaded on PANGAEA (https://doi.org/10.1594/PANGAEA.981128, Zuhr et al., 2026a) as well as the TWT and SMB information for all five IRHs (https://doi.pangaea.de/10.1594/PANGAEA.983767, Zuhr et al., 2026b). Density data of firn core B52 are published on PANGAEA in Frenzel et al. (2026) (https://doi.org/10.1594/PANGAEA.984992). Data from Medley et al. (2018), Medley and Thomas (2019), Eswaran et al. (2024) and Winton et al. (2024) are derived from the publications and their respective data availability statements.

Acknowledgments
We thank Mathieu Morlighem for handling our manuscript and the two anonymous reviewers for their constructive feedback. We further thank the AWI polar aircraft technicians Eduard Gebhard and Christoph Petersen for their support in the field during the 2023/24 radar campaign, the Kenn Borek Air crew of AWI's polar research aircraft and the staff at the Norwegian station Troll for their support. We acknowledge support via AWI's airborne radar campaign funding Grant AWI_PA_02146. Logistical support in the field has been provided by Troll station (Norway) and Kohnen station. We acknowledge the use of software from Open Polar Radar generated with support from the University of Kansas; NASA Grants 80NSSC20K1242 and 80NSSC21K0753; and NSF Grants OPP-2027615, OPP-2019719, OPP-1739003, IIS-1838230, RISE-2126503, RISE-2127606, and RISE-2126468. The authors would like to thank Aspen Technology, Inc. for providing software licenses and support. Further, we acknowledge the Norwegian Polar Institute's Quantarctica package. Alexandra M. Zuhr was funded by the DFG (German Research Foundation) in the framework of the priority programme SPP 1158 "Antarctic Research with Comparative Investigations in Arctic Ice Areas" (Grant 522419679). Steven Franke was funded by the Walter Benjamin Programme of the Deutsche Forschungsgemeinschaft (DFG; project no. 506043073). We also indicate we used artificial intelligence (AI) tools to improve the English syntax in some sections of the manuscript and for optimizing portions of the code, such as the figure design. Open Access funding enabled and organized by Projekt DEAL.

References

Agosta, C., Amory, C., Kittel, C., Orsi, A., Favier, V., Gallée, H., et al. (2019). Estimation of the Antarctic surface mass balance using the regional climate model MAR (1979–2015) and identification of dominant processes. *The Cryosphere*, *13*(1), 281–296. https://doi.org/10.5194/tc-13-281-2019

Alfred-Wegener-Institut (AWI) Helmholtz-Zentrum für Polar- und Meeresforschung. (2016a). Neumayer III and Kohnen station in Antarctica operated by the Alfred Wegener institute. *Journal of Large-Scale Research Facilities JLSRF*, *2*, 85. https://doi.org/10.17815/jlsrf-2-152

Alfred-Wegener-Institut (AWI) Helmholtz-Zentrum für Polar- und Meeresforschung. (2016b). Polar aircraft Polar5 and Polar6 operated by the Alfred Wegener institute. *Journal of Large-Scale Research Facilities JLSRF*, *2*, 87. https://doi.org/10.17815/jlsrf-2-153

Altnau, S., Schlosser, E., Isaksson, E., & Divine, D. (2015). Climatic signals from 76 shallow firn cores in Dronning Maud Land, East Antarctica. *The Cryosphere*, *9*(3), 925–944. https://doi.org/10.5194/tc-9-925-2015

Anschütz, H., Eisen, O., Oerter, H., Steinhage, D., & Scheinert, M. (2007). Investigating small-scale variations of the recent accumulation rate in coastal Dronning Maud Land, East Antarctica. *Annals of Glaciology*, *46*(1), 14–21. https://doi.org/10.3189/172756407782871756

Anschütz, H., Müller, K., Isaksson, E., McConnell, J. R., Fischer, H., Miller, H., et al. (2009). Revisiting sites of the South Pole Queen Maud Land traverses in East Antarctica: Accumulation data from shallow firn cores. *Journal of Geophysical Research*, *114*(D24). https://doi.org/10.1029/2009JD012204

Anschütz, H., Sinisalo, A., Isaksson, E., McConnell, J. R., Hamran, S.-E., Bisiaux, M. M., et al. (2011). Variation of accumulation rates over the last eight centuries on the East Antarctic Plateau derived from volcanic signals in ice cores. *Journal of Geophysical Research*, *116*(D20), D20103. https://doi.org/10.1029/2011JD015753

Bohling, G. (2005). Introduction to geostatistics and variogram analysis. *Kansas Geological Survey*, *1*(10), 1–20.

Budd, W. F., & Carter, D. B. (1971). An analysis of the relation between the surface and bedrock profiles of ice caps. *Journal of Glaciology*, *10*(59), 197–209. https://doi.org/10.3189/S0022143000013174

Curran, P. J. (1988). The semivariogram in remote sensing: An introduction. *Remote Sensing of Environment*, *24*(3), 493–507. https://doi.org/10.1016/0034-4257(88)90021-1

Dalaiden, Q., Goosse, H., Rezsöhazy, J., & Thomas, E. R. (2021). Reconstructing atmospheric circulation and sea-ice extent in the West Antarctic over the past 200 years using data assimilation. *Climate Dynamics*, *57*(11), 3479–3503. https://doi.org/10.1007/s00382-021-05879-6

Dallmayr, R., Laepple, T., Freitag, J., Behrens, M., Lisovski, S., Jansen, D., et al. (2025). Topographic effect creates non-climatic variations in ice-core based temperature records of the last millennium in Dronning Maud Land, Antarctica. *Geophysical Research Letters*, *52*(9), e2025GL115124. https://doi.org/10.1029/2025GL115124

Dattler, M. E., Lenaerts, J. T. M., & Medley, B. (2019). Significant spatial variability in radar-derived West Antarctic accumulation linked to surface winds and topography. *Geophysical Research Letters*, *46*(22), 13126–13134. https://doi.org/10.1029/2019GL085363

Drews, R., Matsuoka, K., Martín, C., Callens, D., Bergeot, N., & Pattyn, F. (2015). Evolution of Derwael ice rise in Dronning Maud Land, Antarctica, over the last millennia. *Journal of Geophysical Research: Earth Surface*, *120*(3), 564–579. https://doi.org/10.1002/2014JF003246

Eisen, O., Frezzotti, M., Genthon, C., Isaksson, E., Magand, O., van den Broeke, M. R., et al. (2008). Ground-based measurements of spatial and temporal variability of snow accumulation in East Antarctica. *Reviews of Geophysics*, *46*(2), 2006RG000218. https://doi.org/10.1029/2006RG000218

Eisen, O., Nixdorf, U., Wilhelms, F., & Miller, H. (2004). Age estimates of isochronous reflection horizons by combining ice core, survey, and synthetic radar data. *Journal of Geophysical Research*, *109*(B4), 2003JB002858. https://doi.org/10.1029/2003JB002858

Eisen, O., Rack, W., Nixdorf, U., & Wilhelms, F. (2005). Characteristics of accumulation around the EPICA deep-drilling site in Dronning Maud Land, Antarctica. *Annals of Glaciology*, *41*, 41–46. https://doi.org/10.3189/172756405781813276

Eisen, O., Steinhage, D., Franke, S., Helm, V., Binder, T., Drews, R., et al. (2024). Collection of datasets from AWI's radio-echo sounding systems on ice sheets and glaciers [Dataset]. *PANGAEA*. https://doi.org/10.1594/PANGAEA.972094

Eswaran, A., Truax, O. J., & Fudge, T. J. (2024). 20th-Century Antarctic Sea level mitigation driven by uncertain East Antarctic accumulation history. *Geophysical Research Letters*, *51*(9), e2023GL106991. https://doi.org/10.1029/2023GL106991

Franke, S., Steinhage, D., Helm, V., Binder, T., Nixdorf, U., Miller, H., et al. (2025). Review article: 30 years of airborne radar surveys on the Antarctic and Greenland ice sheets by the Alfred Wegener Institute. *EGUsphere* [preprint]. https://doi.org/10.5194/egusphere-2025-5328

Franke, S., Steinhage, D., Helm, V., Zuhr, A. M., Bodart, J. A., Eisen, O., & Bons, P. (2025). Age–depth distribution in western Dronning Maud Land, east Antarctica, and Antarctic-wide comparisons of internal reflection horizons. *The Cryosphere*, *19*(3), 1153–1180. https://doi.org/10.5194/tc-19-1153-2025

Frenzel, A., Freitag, J., Laepple, T., Zuhr, A., & Kipfstuhl, S. (2026). Density of firn core B52 [Dataset]. *PANGAEA*. https://doi.org/10.1594/PANGAEA.984992

Fretwell, P., Pritchard, H. D., Vaughan, D. G., Bamber, J. L., Barrand, N. E., Bell, R., et al. (2013). Bedmap2: Improved ice bed, surface and thickness datasets for Antarctica. *The Cryosphere*, *7*(1), 375–393. https://doi.org/10.5194/tc-7-375-2013

Frieler, K., Clark, P. U., He, F., Buizert, C., Reese, R., Ligtenberg, S. R. M., et al. (2015). Consistent evidence of increasing Antarctic accumulation with warming. *Nature Climate Change*, *5*(4), 348–352. https://doi.org/10.1038/nclimate2574

Fudge, T. J., Markle, B. R., Cuffey, K. M., Buizert, C., Taylor, K. C., Steig, E. J., et al. (2016). Variable relationship between accumulation and temperature in West Antarctica for the past 31,000 years. *Geophysical Research Letters*, *43*(8), 3795–3803. https://doi.org/10.1002/2016GL068356

Fujita, S., Holmlund, P., Andersson, I., Brown, I., Enomoto, H., Fujii, Y., et al. (2011). Spatial and temporal variability of snow accumulation rate on the East Antarctic ice divide between Dome Fuji and EPICA DML. *The Cryosphere*, *5*(4), 1057–1081. https://doi.org/10.5194/tc-5-1057-2011

Hirsch, N., Zuhr, A. M., Münch, T., Hörhold, M., Freitag, J., Dallmayr, R., & Laepple, T. (2023). Stratigraphic noise and its potential drivers across the plateau of Dronning Maud Land, East Antarctica. *The Cryosphere*, *17*(10), 4207–4221. https://doi.org/10.5194/tc-17-4207-2023

Hofstede, C. M., Roderik, S. W. W., Kaspers, K. A., Broeke, M. R., Karlöf, L., Winther, J.-G., et al. (2004). Firn accumulation records for the past 1000 years on the basis of dielectric profiling of six cores from Dronning Maud Land, Antarctica. *Journal of Glaciology*, *50*(169), 279–291. https://doi.org/10.3189/172756504781830169

IPCC. (2023). Climate change 2023: Synthesis report. Summary for policymakers. Contribution of working groups I, II and III to the sixth assessment report of the intergovernmental panel on climate change.

Karlöf, L., Isaksson, E., Winther, J.-G., Gundestrup, N., Meijer, H. A., Mulvaney, R., et al. (2005). Accumulation variability over a small area in east Dronning Maud Land, Antarctica, as determined from shallow firn cores and snow pits: Some implications for ice-core records. *Journal of Glaciology*, *51*(174), 343–352. https://doi.org/10.3189/172756505781829232

Karlöf, L., Winther, J.-G., Isaksson, E., Kohler, J., Pinglot, J. F., Wilhelms, F., et al. (2000). A 1500 year record of accumulation at Amundsenisen western Dronning Maud Land, Antarctica, derived from electrical and radioactive measurements on a 120 m ice core. *Journal of Geophysical Research*, *105*(D10), 12471–12483. https://doi.org/10.1029/1999JD901119

Kittel, C., Amory, C., Agosta, C., Jourdain, N. C., Hofer, S., Delhasse, A., et al. (2021). Diverging future surface mass balance between the Antarctic ice shelves and grounded ice sheet. *The Cryosphere*, *15*(3), 1215–1236. https://doi.org/10.5194/tc-15-1215-2021

Koch, I., Drews, R., Franke, S., Jansen, D., Oraschewski, F. M., Muhle, L. S., et al. (2023). Radar internal reflection horizons from multisystem data reflect ice dynamic and surface accumulation history along the Princess Ragnhild Coast, Dronning Maud Land, East Antarctica. *Journal of Glaciology*, *70*, 1–19. https://doi.org/10.1017/jog.2023.93

Medley, B., Joughin, I., Das, S. B., Steig, E. J., Conway, H., Gogineni, S., et al. (2013). Airborne-radar and ice-core observations of annual snow accumulation over Thwaites Glacier, West Antarctica confirm the spatiotemporal variability of global and regional atmospheric models. *Geophysical Research Letters*, *40*(14), 3649–3654. https://doi.org/10.1002/grl.50706

Medley, B., McConnell, J. R., Neumann, T. A., Reijmer, C. H., Chellman, N., Sigl, M., & Kipfstuhl, S. (2018). Temperature and snowfall in Western Queen Maud Land increasing faster than climate model projections. *Geophysical Research Letters*, *45*(3), 1472–1480. https://doi.org/10.1002/2017GL075992

Medley, B., & Thomas, E. R. (2019). Increased snowfall over the Antarctic Ice Sheet mitigated twentieth-century sea-level rise. *Nature Climate Change*, *9*(1), 34–39. https://doi.org/10.1038/s41558-018-0356-x

Monaghan, A. J., Bromwich, D. H., Fogt, R. L., Wang, S.-H., Mayewski, P. A., Dixon, D. A., et al. (2006). Insignificant change in Antarctic snowfall since the international geophysical year. *Science*, *313*(5788), 827–831. https://doi.org/10.1126/science.1128243

Morlighem, M., Rignot, E., Binder, T., Blankenship, D., Drews, R., Eagles, G., et al. (2020). Deep glacial troughs and stabilizing ridges unveiled beneath the margins of the Antarctic ice sheet. *Nature Geoscience*, *13*(2), 132–137. https://doi.org/10.1038/s41561-019-0510-8

Mottram, R., Hansen, N., Kittel, C., van Wessem, J. M., Agosta, C., Amory, C., et al. (2021). What is the surface mass balance of Antarctica? An intercomparison of regional climate model estimates. *The Cryosphere*, *15*(8), 3751–3784. https://doi.org/10.5194/tc-15-3751-2021

Müller, K., Sinisalo, A., Anschütz, H., Hamran, S.-E., Hagen, J.-O., McConnell, J. R., & Pasteris, D. R. (2010). An 860 km surface mass-balance profile on the East Antarctic plateau derived by GPR. *Annals of Glaciology*, *51*(55), 1–8. https://doi.org/10.3189/172756410791392718

Nicola, L., Notz, D., & Winkelmann, R. (2023). Revisiting temperature sensitivity: How does Antarctic precipitation change with temperature? *The Cryosphere*, *17*(7), 2563–2583. https://doi.org/10.5194/tc-17-2563-2023

Oerter, H., Graf, W., Wilhelms, F., Minikin, A., & Miller, H. (1999). Accumulation studies on Amundsenisen, Dronning Maud Land, Antarctica, by means of tritium, dielectric profiling and stable-isotope measurements: First results from the 1995–96 and 1996–97 field seasons. *Annals of Glaciology*, *29*, 1–9. https://doi.org/10.3189/172756499781820914

Oerter, H., Wilhelms, F., Jung-Rothenhäusler, F., Göktas, F., Miller, H., Graf, W., & Sommer, S. (2000). Accumulation rates in Dronning Maud Land, Antarctica, as revealed by dielectric-profiling measurements of shallow firn cores. *Annals of Glaciology*, *30*, 27–34. https://doi.org/10.3189/172756400781820705

Payne, A. J., Nowicki, S., Abe-Ouchi, A., Agosta, C., Alexander, P., Albrecht, T., et al. (2021). Future Sea level change under coupled model Intercomparison Project phase 5 and phase 6 scenarios from the Greenland and antarctic ice sheets. *Geophysical Research Letters*, *48*(16), e2020GL091741. https://doi.org/10.1029/2020GL091741

Pritchard, H. D., Fretwell, P. T., Fremand, A. C., Bodart, J. A., Kirkham, J. D., Aitken, A., et al. (2025). Bedmap3 updated ice bed, surface and thickness gridded datasets for Antarctica. *Scientific Data*, *12*(1), 414. https://doi.org/10.1038/s41597-025-04672-y

Robinson, E. S. (1966). On the relationship of ice-surface topography to bed topography on the south polar Plateau. *Journal of Glaciology*, *6*(43), 43–54. https://doi.org/10.3189/S0022143000019055

Rotschky, G., Eisen, O., Wilhelms, F., Nixdorf, U., & Oerter, H. (2004). Spatial distribution of surface mass balance on Amundsenisen plateau, Antarctica, derived from ice-penetrating radar studies. *Annals of Glaciology*, *39*, 265–270. https://doi.org/10.3189/172756404781814618

Rotschky, G., Holmlund, P., Isaksson, E., Mulvaney, R., Oerter, H., Broeke, M. R. V. D., & Winther, J.-G. (2007). A new surface accumulation map for western Dronning Maud Land, Antarctica, from interpolation of point measurements. *Journal of Glaciology*, *53*(182), 385–398. https://doi.org/10.3189/002214307783258459

Seroussi, H., Nowicki, S., Payne, A. J., Goelzer, H., Lipscomb, W. H., Abe-Ouchi, A., et al. (2020). ISMIP6 Antarctica: A multi-model ensemble of the Antarctic ice sheet evolution over the 21st century. *The Cryosphere*, *14*(9), 3033–3070. https://doi.org/10.5194/tc-14-3033-2020

Seroussi, H., Pelle, T., Lipscomb, W. H., Abe-Ouchi, A., Albrecht, T., Alvarez-Solas, J., et al. (2024). Evolution of the Antarctic ice sheet over the next three centuries from an ISMIP6 model ensemble. *Earth's Future*, *12*(9), e2024EF004561. https://doi.org/10.1029/2024EF004561

Smith, B., Fricker, H. A., Gardner, A. S., Medley, B., Nilsson, J., Paolo, F. S., et al. (2020). Pervasive ice sheet mass loss reflects competing ocean and atmosphere processes. *Science*, *368*(6496), 1239–1242. https://doi.org/10.1126/science.aaz5845

Studinger, M., Medley, B. C., Brunt, K. M., Casey, K. A., Kurtz, N. T., Manizade, S. S., et al. (2020). Temporal and spatial variability in surface roughness and accumulation rate around 88°S from repeat airborne geophysical surveys. *The Cryosphere*, *14*(10), 3287–3308. https://doi.org/10.5194/tc-14-3287-2020

Thomas, E. R., Van Wessem, J. M., Roberts, J., Isaksson, E., Schlosser, E., Fudge, T. J., et al. (2017). Regional Antarctic snow accumulation over the past 1000 years. *Climate of the Past*, *13*(11), 1491–1513. https://doi.org/10.5194/cp-13-1491-2017

van Dalum, C., van de Berg, W. J., & van den Broeke, M. (2024). Monthly RACMO2.4p1 data for Antarctica (11 km) for SMB, SEB and near-surface variables (1979-2023). *Zenodo*. https://doi.org/10.5281/zenodo.14217232

van Dalum, C., van de Berg, W. J., van den Broeke, M. R., & van Tiggelen, M. (2025). The surface mass balance and near-surface climate of the Antarctic ice sheet in RACMO2.4p1. *The Cryosphere*, *19*(9), 4061–4090. https://doi.org/10.5194/tc-19-4061-2025

Van Liefferinge, B., Taylor, D., Tsutaki, S., Fujita, S., Gogineni, P., Kawamura, K., et al. (2021). Surface mass balance controlled by local surface slope in inland Antarctica: Implications for ice-sheet mass balance and oldest ice delineation in Dome Fuji. *Geophysical Research Letters*, *48*(24), e2021GL094966. https://doi.org/10.1029/2021GL094966

Velicogna, I., Mohajerani, Y., A, G., Landerer, F., Mouginot, J., Noel, B., et al. (2020). Continuity of ice sheet mass loss in Greenland and Antarctica from the GRACE and GRACE Follow-On missions. *Geophysical Research Letters*, *47*(8), e2020GL087291. https://doi.org/10.1029/2020GL087291

Waddington, E. D., Neumann, T. A., Koutnik, M. R., Marshall, H.-P., & Morse, D. L. (2007). Inference of accumulation-rate patterns from deep layers in glaciers and ice sheets. *Journal of Glaciology*, *53*(183), 694–712. https://doi.org/10.3189/002214307784409351

Wang, D., Ma, H., Li, X., Hu, Y., Hu, Z., An, C., et al. (2025). Sustained decrease in inland East Antarctic surface mass balance between 2005 and 2020. *Nature Geoscience*, *18*(6), 462–470. https://doi.org/10.1038/s41561-025-01699-z

Wang, W., Shen, Y., Chen, Q., Wang, F., & Yu, Y. (2025). Spatiotemporal mass change rate analysis from 2002 to 2023 over the Antarctic ice sheet and four glacier basins in Wilkes-Queen Mary Land. *Science China Earth Sciences*, *68*(4), 1086–1099. https://doi.org/10.1007/s11430-024-1517-1

Wang, Y., Ding, M., Reijmer, C. H., Smeets, P. C. J. P., Hou, S., & Xiao, C. (2021). The AntSMB dataset: A comprehensive compilation of surface mass balance field observations over the Antarctic Ice Sheet. *Earth System Science Data*, *13*(6), 3057–3074. https://doi.org/10.5194/essd-13-3057-2021

Wang, Y., & Xiao, C. (2023). An increase in the Antarctic surface mass balance during the past three centuries, dampening global Sea level rise. *Journal of Climate*, *36*(23), 8127–8138. https://doi.org/10.1175/JCLI-D-22-0747.1

Wessem, J. M. V., Reijmer, C. H., Morlighem, M., Mouginot, J., Rignot, E., Medley, B., et al. (2014). Improved representation of East Antarctic surface mass balance in a regional atmospheric climate model. *Journal of Glaciology*, *60*(222), 761–770. https://doi.org/10.3189/2014JoG14J051

Winton, V. H. L., Mulvaney, R., Savarino, J., Clem, K. R., & Frey, M. M. (2024). Drivers of late Holocene ice core chemistry in Dronning Maud Land: The context for the ISOL-ICE project. *Climate of the Past*, *20*(5), 1213–1232. https://doi.org/10.5194/cp-20-1213-2024

Wirths, C., Stocker, T. F., & Sutter, J. C. R. (2024). The influence of present-day regional surface mass balance uncertainties on the future evolution of the Antarctic Ice Sheet. *The Cryosphere*, *18*(9), 4435–4462. https://doi.org/10.5194/tc-18-4435-2024

Zuhr, A., Franke, S., Steinhage, D., & Helm, V. (2026a). Ant 2023/24: AWI airborne ultra-wideband radar data over the plateau area in western Dronning Maud Land, East Antarctica (SnACC DML project) [Dataset]. *PANGAEA*. https://doi.org/10.1594/PANGAEA.981128

Zuhr, A., Franke, S., Steinhage, D., & Helm, V. (2026b). Internal Reflection Horizons (IRHs) in western Dronning Maud Land, East Antarctica, from airborne radar surveys (1209 to 2023) [Dataset]. *PANGAEA*. https://doi.org/10.1594/PANGAEA.983767

Zuhr, A. M., Münch, T., Steen-Larsen, H. C., Hörhold, M., & Laepple, T. (2021). Local-scale deposition of surface snow on the Greenland ice sheet. *The Cryosphere*, *15*(10), 4873–4900. https://doi.org/10.5194/tc-15-4873-2021

Zuhr, A. M., Wahl, S., Steen-Larsen, H. C., Hörhold, M., Meyer, H., & Laepple, T. (2023). A snapshot on the buildup of the stable water isotopic signal in the upper snowpack at EastGRIP on the Greenland ice sheet. *Journal of Geophysical Research: Earth Surface*, *128*(2), e2022JF006767. https://doi.org/10.1029/2022JF006767

References From the Supporting Information

Bingham, R. G., Bodart, J. A., Cavitte, M. G. P., Chung, A., Sanderson, R. J., Sutter, J. C. R., et al. (2025). Review article: AntArchitecture – Building an age–depth model from Antarctica's radiostratigraphy to explore ice-sheet evolution. *The Cryosphere*, *19*(10), 4611–4655. https://doi.org/10.5194/tc-19-4611-2025

Frezzotti, M., Scarchilli, C., Becagli, S., Proposito, M., & Urbini, S. (2013). A synthesis of the Antarctic surface mass balance during the last 800 yr. *The Cryosphere*, *7*(1), 303–319. https://doi.org/10.5194/tc-7-303-2013

Hale, R., Miller, H., Gogineni, S., Yan, J. B., Rodriguez-Morales, F., Leuschen, C., et al. (2016). Multi-Channel ultra-wideband radar sounder and imager. *2016 IEEE International Geoscience and Remote Sensing Symposium (IGARSS)*, 2112–2115. https://doi.org/10.1109/igarss.2016.7729545

Kovacs, A., Gow, A. J., & Morey, R. M. (1995). The in-situ dielectric constant of polar firn revisited. *Cold Regions Science and Technology*, *23*(3), 245–256. https://doi.org/10.1016/0165-232x(94)00016-q

Laepple, T., Hörhold, M., Münch, T., Freitag, J., Wegner, A., & Kipfstuhl, S. (2016). Layering of surface snow and firn at Kohnen Station, Antarctica: Noise or seasonal signal? Layering of Antarctic Surface Firn. *Journal of Geophysical Research: Earth Surface*, *121*(10), 1849–1860. https://doi.org/10.1002/2016JF003919

Münch, T., Kipfstuhl, S., Freitag, J., Meyer, H., & Laepple, T. (2017). Constraints on post-depositional isotope modifications in East Antarctic firn from analysing temporal changes of isotope profiles. *The Cryosphere*, *11*(5), 2175–2188. https://doi.org/10.5194/tc-11-2175-2017

Open Polar Radar. (2023). Open Polar Radar. opr (Version 3.0.1) [Computer software]. Retrieved from https://gitlab.com/openpolarradar/opr/doi:10.5281/zenodo.5683959

Sugiyama, S., Enomoto, H., Fujita, S., Fukui, K., Nakazawa, F., Holmlund, P., & Surdyk, S. (2012). Snow density along the route traversed by the Japanese-Swedish Antarctic Expedition 2007/08. *Journal of Glaciology*, *58*(209), 529–539. https://doi.org/10.3189/2012JoG11J201

Weinhart, A. H., Freitag, J., Hörhold, M., Kipfstuhl, S., & Eisen, O. (2020). Representative surface snow density on the East Antarctic Plateau. *The Cryosphere*, *14*(11), 3663–3685. https://doi.org/10.5194/tc-14-3663-2020